

Power System Security Enhancement using FACTS devices in a Power System Network with Voltage Dependent Loads and ZIP Loads

T.A. Ramesh Kumar
Assistant Professor,
Department of Electrical Engineering,
Annamalai University,
Chidambaram, India.

I.A. Chidambaram
Professor,
Department of Electrical Engineering,
Annamalai University,
Chidambaram, India.

ABSTRACT

This paper deals with the overview of a control strategies for power system security assessment of an interconnected power system coordinated with different loads Which is being governed using Flexible AC Transmission system (FACTS) devices when the system is approaching an extreme emergency state. FACTS controllers can be employed to enhance power system stability in addition to their main function of power flow control. In this method, the island is prevented from the total loss of supply using few FACTS devices. The optimization process is carried out using bacterial foraging optimization algorithm. The optimized result exhibits tremendous improvement in the system performance. The proposed scheme is adopted in IEEE 14 bus test system.

Keywords

Flexible AC Transmission System (FACTS), SVC (Static Voltage Control), UPFC (Unified Power Flow Controller), Interline Power Flow Controller (IPFC), VDI (Voltage dependent load), ZIP load, Dynamic Security Assessment (DSA).

1. INTRODUCTION

Power system security refers to the degree of risk in a power systems ability to survive imminent disturbances and, hence, depends on the system operating condition as well as the contingent probability of disturbance. Security assessment is an important study which has to be carried out in an energy management system to determine the security and stability of the system under unfrozen contingencies. Power systems are being operated closer to the stability limit nowadays with several new economic objectives for operation. As power transactions increase, weak connections, unexpected events, and hidden failures in protection systems, human errors and other reasons may cause the system to lose balance and even lead to catastrophic failures. Since late 1960s, power system industries have undertaken considerable effort to develop and implement preventive and corrective measures to reduce the possibility and extent of system outage. Several techniques had been adopted to plan the power system restoration improvement. But with the advent and usage of the FACTS devices like SVC, UPFC, IPFC have made the system restoration significantly improved along with combined effort of system analysts, operating personal and the concurrent use of on-line and off-line computer facilities at the operating center. Any large disruption in generation and load balance in a massively interconnected system can lead to undesirable variations in power flows and bus voltages. Occasionally, this imbalance can spread uncontrollably over an entire system causing blackout of large parts of the system. As the digital age prevails, more efficient manufacturing processes, based

on computers and power electronics, have come to dominate the power industry.

This paper discusses a vision for state-of-the-art solutions to improve power system restoration through -improved monitoring and control. the demand for larger power transf.ers over longer-distances, insufficient investment in the transmission system, exacerbated by continued load growth are the trust areas which require continuous reforms to ensure a quality of power system to the consumers. Wide-Area Monitoring and control tools, Phasor Measurement Units (PMU), Flexible AC Transmission System (FACTS) devices, distributed generation and storage devices are the primary technologies used to address such problems. When a power system is subjected to large disturbances, such as simultaneous loss of several generating units or major transmission lines, and the vulnerability analysis indicates that the system is approaching a catastrophic failure, control actions has to be taken to limit the extent of the disturbances.

The basic restoration assessment for Voltage Dependent Load (VDL)/ ZIP Loads in the power system network has been carried out and the various control corrective actions using several FACTS devices are considered for the power system security enhancement.

2 DYNAMIC SECURITY ASSESSMENT

DSA refers to the analysis required to determine whether the power system can meet specified reliability and security criteria in both transient and steady-state time frames for all credible contingencies. In the operating environment, a secure system is one in which operating criteria are respected at pre- and post contingency conditions. This implies that analyses must be performed to assess all aspects of security, including the thermal loading of system elements, voltage and frequency variations (both steady state and transient), and all forms of stability.

Due to the nature of the disturbance and the set up of the power system network, there are two main elements in the Power System Security Assessment, Static Security Assessment and Dynamic Security Assessment [1]. Static Security Assessment is usually performed prior to dynamic security assessment. If the analysis evaluates only the expected post disturbance equilibrium condition (steady-state operating point), this is referred as Static Security Assessment (SSA). Static security is related to an equilibrium point of the system, where voltage and thermal limits are observed. It neglects the transient behavior and any other time dependent variations caused by changes in load conditions [2].

If the analysis evaluates the transient performance of the system as it progresses after the disturbance, this is referred as Dynamic Security Assessment (DSA). Dynamic Security Assessment is an evaluation of the ability of a power system

to withstand a defined set of contingencies and to survive the transition to an acceptable steady-state condition..

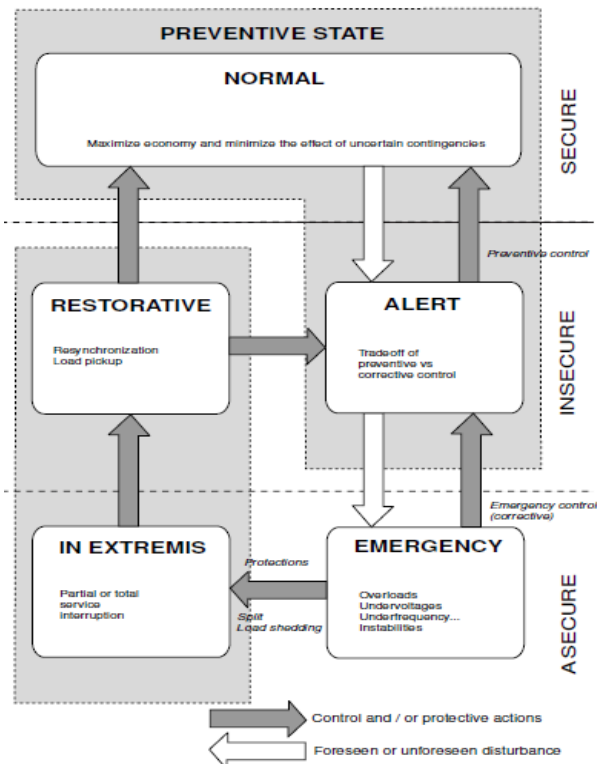


Fig 1: The operating states and transitions for power

If the system is secured, these oscillations will decay and has to be damped out eventually. Otherwise, the oscillation of the frequency and voltage will grow to the extent of shutting down the generator. If the disturbance is small, which means that the voltage only oscillates close to the equilibrium point, it is then appropriate to examine the Eigen values of a linear version of the system model. If the system experiences a major disturbance, the oscillation will keep growing to a significant magnitude. The stability is then measured based on the trajectories of the disturbed systems motion related to the region of attraction of the final equilibrium state. For such situations, the use of nonlinear system model and the analysis theory for nonlinear system are required. The transient stability depends on the magnitude of the fault, duration of the fault and the speed of the protective devices. If the system is transiently stable, the oscillation of the rotor angle will damp down to a safe operating limit. Due to the tremendous growth in the interconnected Power system network with more complicated load models, increase the possibility of disturbance occurrences and the propagation of the disturbance. So the concept of the preventive (normal), emergency, and restorative operating states and their associated controls are to be adopted effectively.

Very early power systems were often separate and isolated regions of generators and loads. As systems became larger and more interconnected, the possibility of disturbances propagating long distance is increased. The concept of the preventive (normal), emergency, and restorative operating states and their associated controls are shown in Fig. 1. The preventive state is the normal state wherein the system is stable with all components within operating constraints. The emergency state arises when the system begins to lose stability, or when component operating constraints are violated. The restorative state is when service to some

customers has been lost, usually due to progression through the emergency state and the operation of protective devices.

2.1 Off-Line DSA

In off-line DSA analysis, detailed time-domain stability analysis is performed for all credible contingencies and a variety of operating conditions. In most cases, this off-line analysis is used to determine limits of power transfers across important system interfaces[5]. These limits then are used in an operating environment that is hopefully not significantly different from those conditions considered. Since the analysis is performed off-line, there is not a severe restriction on computation time and therefore detailed analysis can be done for a wide range of conditions and contingencies. These studies include numerical integration of the models for a

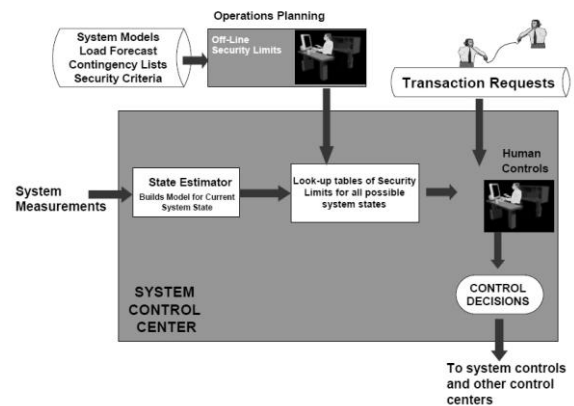


Fig 2: Traditional Off-line Security Assessment

certain proposed power transfer condition and for a list of contingencies typically defined by a faulted location and specified fault-clearing time (based on known relay settings).The trajectories of the simulation are analyzed to find if voltage transients are acceptable, and to verify whether the transient stability is maintained during the specified fault-clearing time.

If the results for one level of power transfer are acceptable for all credible contingencies, the level of proposed power transfer is increased and the analysis is repeated. This process continues until the level of power transfer reaches a point where the system cannot survive all of the credible contingencies. The maximum allowable transfer level is then fixed at the last acceptable level, or reduced by some small amount to provide a margin that would account for changes in conditions when the actual limit is in force.

MATHEMATICAL MODEL OF DYNAMIC SECURITY ASSESSMENT

The dynamic behavior of multi-machine power system is described by the detailed modeling of all the elements of the power system [3].

$$M \frac{d^2 \delta}{dt^2} + D \frac{d\delta}{dt} + P_{ei} = P_{mi} \quad (1)$$

$$\frac{d\delta_0}{dt} = \omega_0 \quad (2)$$

The general relation for dynamic behavior of a multi-machine power system used for both dynamic and transient security assessment be represented as

$$P_{ei} = E_i \sum_{j=1}^{N_g} E_j [G_{ij} \cos(\delta_0 - \delta_1) + B_{ij} \sin(\delta_i - \delta_j)] \quad (3)$$

Where $i = 1, 2, \dots, N_g$, D_i are the inertia and damping constant of the i_{th} generation; P_{mi} mechanical input to the i_{th} generator; E_j is the EMF behind X'_{di} of the i_{th} generator; G_{ij} , B_{ij} are the real and imaginary parts of the admittance matrix of the of the reduced system, X'_{di} is the transient reactance of the i_{th} generator; N_g is the number of synchronous generator in the system. Modification of equ (3) for dynamic security assessment could result as

$$\frac{Md^2 \delta}{dt^2} = P_{mi} - P_{ei} = P_m - P_{maxi} \quad (4)$$

4. MODELLING OF LOADS

A load model can be mathematically represented with the relationship between power and voltage, where the power is either active or reactive and the output from the model. The voltage (magnitude and/or frequency) is the input to the model. The load model could be a static or dynamic load model or a combination of both. Load models are used for analyzing power system stability problems, such as steady state stability, transient stability, long term stability and voltage control. According to the power voltage equation, power system loads are divided into constant-impedance, constant power and constant current loads. A considerable amount of loads in power systems are induction motors. All the induction motors connected to a busbar may be modelled as a single motor, parameters of which are obtained from the parameters of all motors which is referred as dynamic load modelling. [4].

5. DYNAMIC LOAD MODELS

The dynamic load model describes the time dependence as well as the voltage dependence of the load. The characteristic of a bus load depends on the load composition, which means that the aggregated load characteristics for the bus load must be found. These load parameters can be derived by a field measurement based method. And this method is based on direct measurement at a bus, during system disturbances or planned system disturbances, where voltage, frequency, active power and reactive power are measured and then a method, such as the *Least Square Method* is used to derive parameters to the aggregated load model.

Field Measurement Based Method

- Straightaway simply measure and derive a model.
- Unless the load composition is analysed in some detail and unless buses having loads of fairly different compositions are measured there will be no understanding of the results so that they can be extrapolated to different conditions.
- Spontaneous load variations are included in the load model, especially during long term measurements. [5]

A major challenge remained always in finding the numerical values for voltage dependency and frequency dependency; however, this has been successfully achieved in Germany. Traditionally, lumped feeder loads are represented as static composite load models on the basis of constant impedance (Z), constant current (I) or constant power (P) contributions, also called ZIP-loads. Further improvements of these models resulted in a classical dynamic model that was, however, still linear in its voltage and frequency dependence of active and reactive power. To overcome the drawbacks of linearity,

Kermendey et al. proposed in [5] a more advanced load model The model contained of a static part being purely dependent on supply voltage and load current, realised by a voltage dependent impedance.

5.1 Mathematical Model of Dynamic Loads

The General form of Load Modelling equation can be written as,[5]

$$\dot{x} = a(x, v) \quad (7)$$

$$P_H = b_p(x, v) \quad (8)$$

$$Q_H = b_q(x, v) \quad (9)$$

The equation for active load power are given, However similar equations are hold for reactive load power.

$$P_H = b_p(X(\infty), v) \quad (10)$$

Where $x(\infty)$ solve $\dot{x} = 0$, ie $a(x, v) = 0$ for static load characteristic and,

$$P_H = b_p(X(0), v) \quad (11)$$

Where $x(0)$ is the value of the state when the initial change occurs. Dynamic load model with exponential recovery, propose in [6], Load characteristic are constant power in steady state and transient during constant impedance. A simple dynamic load model based on the response to a voltage steps, it is a useful approximation that the recovery is exponential [6]. A differential equation that defines the behaviour is:

$$T_p \dot{P}_H + P_H = P_s(V) + k_p(V) \dot{V} \quad (10)$$

This equation can be written in first-order form as:

$$\dot{X}_p = P_s(V) - P_L \quad (11)$$

$$P_H = \frac{\dot{X}_p}{T_p} + P_t(V) \quad (12)$$

Where T_p is the time constant X_p is a state variable, $P_s(V)$ is the static load function and $P_t(V)$ is the transient load function. By using this form of differential equation, for active as well as reactive power, the system voltage can be determined after the disturbance [7].

5.1.1. Voltage Dependent Load (VDL)

Voltage Dependent Loads (VDL) are nonlinear load model which represents the power relationship to voltage as an exponential equation. The load powers P_H and Q_H are preceded as negative power as these powers are absorbed from the bus, as follows:

$$-P_H = P_0 (v/v_0)^{2p} \quad (13)$$

$$-Q_H = Q_0 (v/v_0)^{2q} \quad (14)$$

Where v_0 is the initial voltage at the load bus as obtained by the power flow solution. The parameters of this model are γ_p , γ_q , and the values of the active and reactive power, P_0 and Q_0 , at the initial conditions. Common values for the exponents of

the model for different load components γ_p and γ_q are (0, 1, 2). Equations can be directly included in the formulation of power flow analysis. However, VDLs are generally initialized after the power flow analysis, and P_0 and Q_0 are computed based on constant PQ load powers p_{L0} and q_{L0} . In this case, the initial voltage is not known V_0 , the following equation can be used,

$$P = P_0 V^{\gamma_p} \quad (15)$$

$$Q = Q_0 V^{\gamma_q} \quad (16)$$

Where the γ_p and γ_q the active and reactive power exponent. The units of P_0 and Q_0 depends on the status parameter k . If $k=1$, the VDL is initialized after the power flow analysis, and P_0 and Q_0 are in percentage of the PQ load power connected at the VDL bus.

$$P_0 = \frac{k_p}{100} P_L \quad (17)$$

$$Q_0 = \frac{k_q}{100} P_L \quad (18)$$

5.1.2. ZIP Load

Polynomial or ZIP loads are the nonlinear load model whose powers are a quadratic expression of the bus voltage. The ZIP model, equations (19) and (20), is a polynomial model that represents the sum of these three categories:

$$-P_H = g \left(\frac{v}{v_0} \right)^2 + I_p \frac{v}{v_0} + P_m \quad (19)$$

$$-Q_H = b \left(\frac{v}{v_0} \right)^2 + I_q \frac{v}{v_0} + Q_m \quad (20)$$

Where v_0 is the initial voltage at the load bus as obtained by the power flow solution. Other parameters of ZIP load is initialized after the power flow analysis [8], the parameters can be defined based on the PQ load powers P_{L0} and Q_{L0} :

$$g = \frac{g}{100} \frac{P_{L0}}{v_0^2}, \quad I_p = \frac{I_p}{100} \frac{P_{L0}}{v_0}, \quad P_m = \frac{P_m}{100} P_{L0}$$

$$b = \frac{b}{100} \frac{Q_{L0}}{v_0^2}, \quad I_q = \frac{I_q}{100} \frac{Q_{L0}}{v_0}, \quad Q_m = \frac{Q_m}{100} Q_{L0}$$

in this case initial voltage V_0 is also not known, thus following equation is used.

$$-P_H = g v^2 + I_p v + P_m \quad (21)$$

$$-Q_H = b v^2 + I_q v + Q_m \quad (22)$$

The parameters are constants and indicate the nominal power is divided into constant power, constant current and constant impedance [7].

5.2 Identification of Model Parameters.

$$P_H = [1 + K_p (V - 1)] (1 - P_{drop}) + P_{dyn} (G.V^2 - 1) \quad (23)$$

$$Q_H = [1 + K_q (V - 1)] (1 - Q_{drop}) + Q_{dyn} (B.V^2 - 1) \quad (24)$$

Considering the model given by equation (23), the nonlinear relationship between the measured signals, active power P , voltage V at the load bus and the estimated conductance G , and the parameters K_p , P_{drop} and P_{dyn} can be simplified by re-parameterization, and the model can be written as a linear regression equation (25)

$$P_H = [x(1) + x(2).(V - 1)] + P_{dyn} (G.V^2 - 1) \quad (25)$$

Where

$$x(1) = (1 - P_{drop}) \quad (26)$$

$$x(2) = x(1).K_p \quad (27)$$

$$z(t) = \gamma^T(t).\theta_p \quad (28)$$

$$\theta_p = (x(1).x(2).P_{dyn}) \quad (29)$$

The Least Squares method has then been used for the identification [8]. The objective is to obtain the best estimates for the parameter vector θ_p , which minimizes the difference between the estimated active power and the simulated one (as a quadratic criterion). With the given equation (23). The same procedure is applied for the parameter identification for the reactive load using equation (24). The augmented objective function to be minimized using a least square criterion which is given by equation (30). The final parameters are determined directly from the expressions given in (26) and (27) The least squares method is used to minimize the function (29) and to obtain the best estimates for the parameter vector θ_p .

$$L(\theta_p) = \sum_{k=1}^N (P_{simulated}(t_k, \theta_p) - P_{measured}(t_k, \theta_p))^2 \quad (30)$$

The same procedure is repeated for the reactive powers also. The optimum solution represents the of the global minimum of the objective function, i.e. the best estimates for the model. However, the nonlinear model parameters can be estimated accurately by an iterative approach whose algorithm is as follows:

* An initial estimate X_0 for the parameters is selected;

* The best fit is then determined by using the initial estimate X_0 ; the best estimates are compared with the initial estimates, and it is determined whether the fit improves or not. The direction and magnitude of the adjustment depend on the fitting algorithm [9].

6. FACTS-DEVICE OVERVIEW

The development of FACTS-devices [10] in ensuring high reliability as well as high efficiency with the modern power electronic components has elaborated the usage in various applications in the power system network. Voltage Source Converters provide a free controllable voltage in magnitude and phase due to pulse width modulation of the IGBTs or IGCTs. High modulation frequencies allow to get low harmonics in the output signal and even to compensate disturbances coming from the network. The disadvantage is that with an increasing switching frequency, the losses are increasing as well. Therefore special designs of the converters are required to compensate this.

7. OPERATION AND MATHAMATICAL MODEL OF FACTS DEVICES

7.1 Static Var Compensator (Svc)

A rapidly operating Static VAR Compensator (SVC) can continuously provide the reactive power required to control dynamic voltage oscillations under various system conditions and thereby improve the power system transmission and distribution stability. Installing an SVC at one or more suitable points in the network can increase transfer capability and reduce losses while maintaining a smooth voltage profile under different network conditions. In addition an SVC can mitigate active power oscillations through voltage amplitude modulation. SVC installations consist of a number of building blocks [11]. And an accurate representation of the SVC droop control during steady-state analysis is important, especially when the SVC is operating close to the limits. In addition, an accurate SVC susceptance or the corresponding firing angle is necessary for various analysis involved in power system design .

7.2. SVC Models in Load Flow Calculations

There are mainly three existing SVC models that can be used in load flow analyses, e.g. the generator-fixed susceptance model, the total susceptance model and the firing angle model.. A characteristic model based on the steady-state characteristic of SVC is presented. In the end, two combined models are developed to improve the accuracy of the total susceptance model and the firing angle model.

In practice the SVC can be seen as an adjustable reactance with either firing angle limits or reactance limits. The circuit shown in Fig. 4 is used to derive the SVC's nonlinear power equations and the Linearized equations required by Newton's method [12].

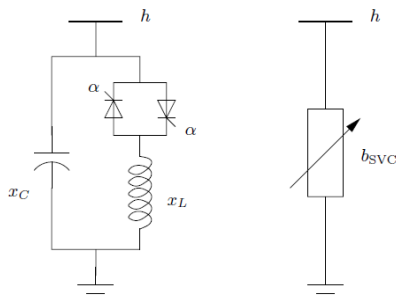


Fig 3: SVC schemes: (a) firing angle model and (b) equivalent susceptance model

In general, a common approximation consists in assuming that the controlled variable is b_{SVC} and not the firing angle α . Thus, the regulator has to vary α in order to control the bus voltage as shown in fig (3). The state variable α undergoes an anti-windup limiter which indirectly allows limiting the SVC current and positive sequence SVC models for Newton- Raphson load flows are presented in this section. The Linearized equation of the SVC is given by,

$$\begin{bmatrix} \Delta P_k \\ \Delta Q_k \end{bmatrix}^i = \begin{bmatrix} 0 & 0 \\ 0 & Q_k \end{bmatrix}^i \begin{bmatrix} \Delta \theta_k \\ \Delta B_{SVC}/B_{SVC} \end{bmatrix} \quad (31)$$

Where the total susceptance B_{SVC} is taken to be the state variable, At the end of iteration i , the variable shunt susceptance B_{SVC} is updated according to that

$$B_{SVC}^{i+1} = B_{SVC}^i + (\Delta B_{SVC}/B_{SVC})^i B_{SVC}^i \quad (32)$$

This changing susceptance represents the total SVC susceptance necessary to maintain the nodal voltage magnitude at the specified value [13]. Once the level of compensation has been determined, the firing angle required to achieve such compensation level can be calculated. This assumes that the SVC is represented by the structure shown in Fig.3. Since the SVC susceptance given by is a transcendental equation, the computation of the firing angle value is determined by iteration. considering the firing angle of SVC also as a the state variable, the Linearized SVC equation is given as,

$$\begin{bmatrix} \Delta P_k \\ \Delta Q_k \end{bmatrix}^i = \begin{bmatrix} 0 & 0 \\ 0 & Q_k \end{bmatrix}^i \begin{bmatrix} \Delta \theta_k \\ \alpha \end{bmatrix}^i \quad (33)$$

Where the total susceptance B_{SVC} is updated according to

that

$$\frac{\partial Q_k}{\partial \alpha} = \frac{2V_k^2}{X_L} (\cos(2\alpha) - 1) \quad (34)$$

At the end of i^{th} iteration, the variable firing angle α is update according to equ (36), $\alpha^{i+1} = \alpha^i + \Delta \alpha^i$ and the new SVC susceptance B_{eq} is calculated from equ (34). It should be remarked that both models, the total susceptance model and the firing angle model observe good numerical properties. However, the former model requires of an additional iterative procedure, after the load flow solution has converged, to determine the firing angle. Hence, their mathematical formulations are quite different.

8. UNIFIED POWER FLOWCONTROLLER (UPFC)

A unified power flow controller (UPFC) among the most promising device in the FACTS devices group. It has the ability to adjust the three control parameters, *i.e.* the bus voltage, transmission line reactance, and phase angle between two buses, either simultaneously or independently [14]. UPFC performs this through the control of the in-phase voltage, quadrature voltage, and shunt compensation UPFC is combination of a static shunt and static series compensators. It acts as a shunt compensating and a phase shifting device simultaneously. The UPFC consists of a shunt and a series transformer, which are connected via two voltage source converters with a common DC-capacitor.

The DC-circuit allows the active power exchange between shunt and series transformer to control the phase shift of the series voltage. The series converter needs to be protected with a Thyristor bridge. Due to the high efforts for the Voltage Source Converters and the protection, an UPFC is getting quite expensive [15], which limits the practical applications where the voltage and power flow control is required simultaneously

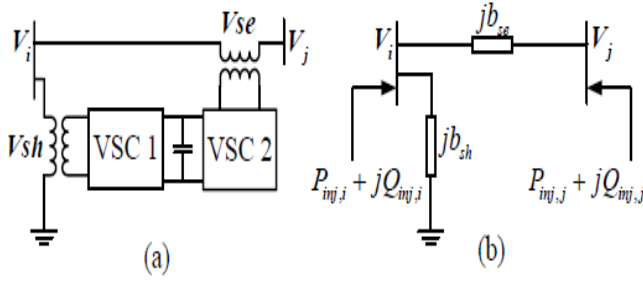


Fig 4: Schematic representation of a two-converter UPFC(a)and its power injection model (b).

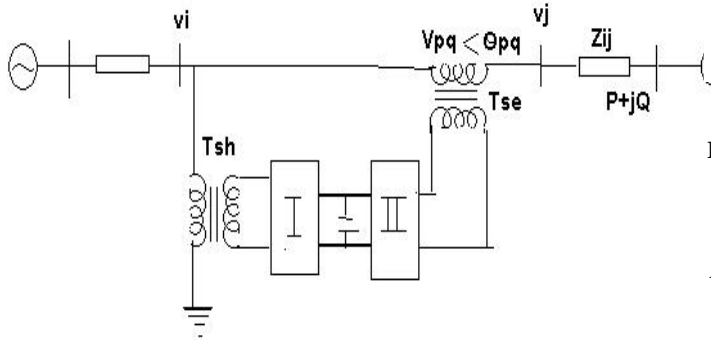


Fig 5: Representation of UPFC

8.1 Steady state UPFC representation:

The UPFC can be represented in steady state by the two voltage sources with appropriate impedance as shown in fig.5, the voltage source can be represented by the relationship between the voltage and amplitude modulation ratios and phase shift of UPFC. In this model the shunt transformer impedance and the transmission line impedance including the series transformer are assumed to be constant. No power loss is considered within the UPFC. However, the proposed model and algorithm can easily include these when required.

8.2 Power injection model of UPFC:

The two voltage source model of the UPFC is converted into power injection model. The advantages of power injection are that it does not destroy the symmetric characteristics of the admittance matrix [16].

STEP1: To transform the shunt side of UPFC into a power injection at bus i only. Thus, (fig. 6)

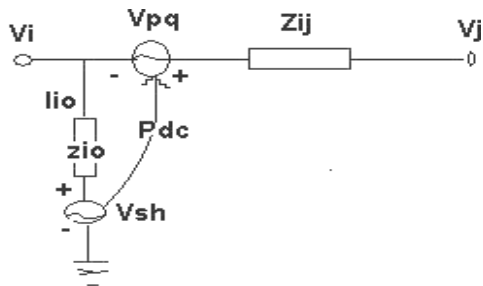


Fig 6: Steady state representation of UPFC

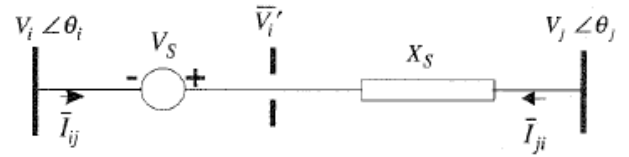


Fig.7: Representation of a series connected VSC

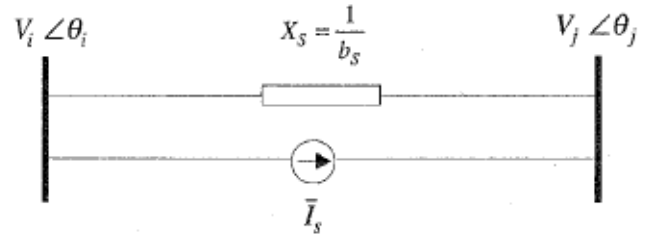


Fig 8: Replacement of a series voltage source by a current source converter.

$$P_{io} = G_{io} * V_i^2 - V_i * G_{io} * \cos(\varphi_{sh} - \delta_i) + V_i * V_{sh} * B_{io} * \sin(\varphi_{sh} - \delta_i) \quad (35)$$

$$Q_{io} = B_{io} * V_i^2 - V_i * G_{io} * \cos(\varphi_{sh} - \delta_i) + V_i * V_{sh} * B_{io} * \sin(\varphi_{sh} - \delta_i) \quad (36)$$

STEP 2: second step is to convert the series source of UPFC into power injection at both bus bar i and j, which is shown in fig 8. Therefore, we have

$$S_i = P_i + jQ_i$$

$$P_i = V_i * V_{pq} * B_{ij} \sin(\theta_{pq} - \delta_i) - V_i * V_{pq} * G_{ij} \cos(\theta_{pq} - \delta_i) \quad (37)$$

$$S_j = P_j + jQ_j$$

$$P_i = V_j * V_{pq} * G_{ij} \cos(\theta_{pq} - \delta_i) - V_j * V_{pq} * B_{ij} \sin(\theta_{pq} - \delta_i) \quad (38)$$

$$Q_i = V_j * V_{pq} * G_{ij} \sin(\theta_{pq} - \delta_i) - V_j * V_{pq} * B_{ij} \cos(\theta_{pq} - \delta_i) \quad (39)$$

But the power transfer from shunt side to series side, is \$P_{dc}\$,

$$P_{dc} = \left(G_{ij} - j B_{ij} \right) \left[V_{pq} \theta_{pq} V_i \begin{matrix} \delta_i + \sqrt{P_{pq}^2} \\ V_{pq} \theta_{pq} V_j - \delta_j \end{matrix} \right] \quad (40)$$

When the power loss inside the UPFC is neglected then \$P_{dc} = P_{io}\$ then, \$P_i = P_i - P_{io}\$; \$Q_i = Q_i - Q_{io}\$ Thus the two power injections (\$P_i, Q_i\$) and (\$P_j, Q_j\$) represents all features of the steady state UPFC model [17].

9. INTERLINE POWER FLOWCONTROLLER (IPFC) AND POWER INJECTION MODEL

When the power flows of two lines to be controlled effectively, an Interline Power Flow Controller (IPFC) which consists of two series VSCs whose DC capacitors are coupled can be coordinated in series with the Tie-line. This allows active power to circulate between the VSCs. Fig.9 (a,b) shows the principle configuration of an IPFC. With this configuration two lines can be controlled simultaneously to optimize the network utilization. In general, due to its complex setup, specific application cases need to be identified justifying the investment [18].

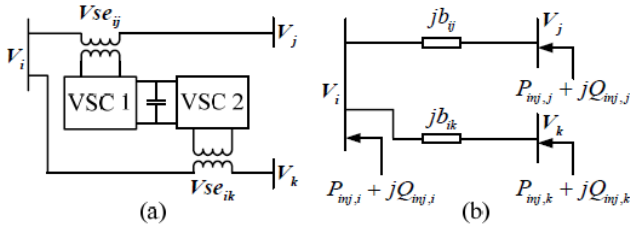


Fig.9: (a) Schematic representation of a two-converter IPFC
(b) Power injection model.

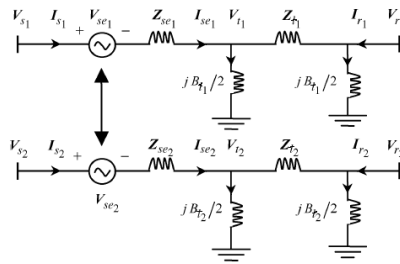


Fig.10: Equivalent circuit of two-converter IPFC using voltage source.

Fig. (10) shows the circuit of an IPFC with two series converters. In this circuit,

The complex Controllable series injected voltage V_{sem}
 $= V_{sem} \angle \theta_{sem}$

Series transformer impedance $Z_{sem} = R_{sem} + jX_{sem}$,
The complex bus voltage at buses s_m and r_m are V_{sm}
 $= V_{sm} \angle \theta_{sm}$, $V_{sm} = V_{sm} \angle \theta_{sm}$,

The line series impedance $Z_{tm} = R_{tm} + jX_{tm}$, and B_{tm} represent the line charging susceptance, respectively [19], m is the line number ($m=1,2,\dots$). From Fig. (10),

$$V_{sm} = V_{sm} + I_{sm} Z_{sem} + V_{tm} \quad (41)$$

$$I_{sm} = \frac{(V_{tm} - V_{rm})}{Z_{tm}} + j \frac{B_{tm}}{2} V_{tm} \quad (42)$$

V_{tm} and I_{sm} can be expressed according to V_{rm} and I_{rm} as

$$V_{tm} = \left(1 + j \frac{B_{tm}}{2} Z_{tm} \right) V_{rm} - I_{rm} Z_{tm} \quad (43)$$

$$I_{sm} = \left(jB_{tm} - j \frac{B_{tm}^2}{4} Z_{tm} \right) V_{rm} - \left(1 + \frac{B_{tm}}{4} Z_{tm} \right) I_{rm} \quad (44)$$

From eqn. (43-46) can be expressed in terms of V_{sm} , V_{rm}

and V_{sem} , I_{sm} and I_{rm} as

$$I_{sm} = \left(A + \frac{SE}{L} \right) V_{rm} + \frac{E}{L} V_{sm} - \frac{E}{L} V_{sem} \quad (45)$$

$$I_{rm} = \frac{S}{L} V_{rm} - \frac{1}{L} V_{sm} + \frac{1}{L} V_{sem} \quad (46)$$

Where

$$A = \left(jB_{tm} - Z_{tm} \frac{B_{tm}^2}{4} \right) \quad E = \left(1 + jZ_{tm} - \frac{B_{tm}}{4} \right)$$

$$S = (Z_{sem} A - E), \quad L = (Z_{sem} E + Z_{tm}),$$

Where V_{sm} , I_{sm} , V_{rm} , I_{rm} , and V_{tm} are the complex bus voltage and current at the corresponding buses s_m and r_m respectively. As IPFC neither absorbs nor injects active power with respect to the ac system [20], the active power exchange between or among the converters via the dc link is zero, and if the resistances of series transformers are neglected, the equation can be written as

$$P_c = \sum_m P_{dm} = 0 \quad (47)$$

Where

$$P_{dm} = R_c (V_{sem} I_{sm}).$$

P_{dm} is a active power exchange on the DC link, V_{sem} is the series injected voltage and I_{sm} complex bus current at bus s_m .

Thus, the power balance equations are as follows

$$P_{gm} + P_{inj,m} - P_{im} - P_{tm} = 0 \quad (48)$$

$$Q_{gm} + Q_{inj,m} - Q_{im} - Q_{tm} = 0 \quad (49)$$

where P_{gm} and Q_{gm} are generated active and reactive powers, P_{lm} and Q_{lm} are load active and reactive powers. $P_{t,m}$ and $Q_{t,m}$, are conventional transmitted active and reactive powers at the bus "i" and "j".

10. BACTERIAL FORAGING OPTIMIZATION ALGORITHM

For over the last five decades, optimization algorithms like Genetic Algorithms (GAs), Evolutionary Programming (EP), Evolutionary Strategies (ES), which draw their inspiration from evolution and natural genetics, have been dominating the realm of optimization algorithms. Recently natural swarm inspired algorithms like Particle Swarm Optimization (PSO),

Ant Colony Optimization (ACO) have found their way into this domain and proved their effectiveness. Bacterial Foraging Optimization Algorithm (BFOA) [21] was proposed by Passion is inspired by the social foraging behavior of *Escherichia coli*. Application of group foraging strategy of a swarm of *E.coli* bacteria in multi-optimal function optimization is the key idea of the new algorithm [22]. Bacteria search for nutrients in a manner to maximize energy obtained per unit time. Individual bacterium also communicates with others by sending signals. A bacterium takes foraging decisions after considering two previous factors.

The process, in which a bacterium moves by taking small steps while searching for nutrients, is called chemo taxis and key idea of BFOA is mimicking Chemotactic movement of virtual bacteria in the problem search space. The control system of these bacteria that dictates how foraging should proceed, can be subdivided into four sections namely Chemotaxis, Swarming, Reproduction, Elimination and Dispersal. These operations among the bacteria are used for searching the total solution space.

10.1. Chemotactic Step

This process is achieved through swimming and tumbling via Flagella. Depending upon the rotation of Flagella in each bacterium, it decides whether it should move in a predefined direction (swimming) or altogether in different directions (tumbling). In BFO algorithm, one moving unit length with random directions represents “tumbling,” and one moving unit length with the same direction relative to the final step represents “swimming.” The chemotactic step consists of one tumbling along with another tumbling, or one tumbling along with one swimming. This movement is can be described as

$$\theta^i(j+1,k,l) = \theta^i(j,l,l) + C(i) \frac{\Delta(i)}{\sqrt{\Delta^T(i)\Delta(i)}} \quad (50)$$

Where C (i) denotes step size ; $\Delta(i)$ Random vector ; $\Delta^T(i)$ Transpose of vector $\Delta(i)$.

10.2. Swarming Step

A group of *E.coli* cells arrange themselves in a traveling ring by moving up the nutrient gradient when placed amidst a semisolid matrix with a single nutrient chemo-effector. The cells when stimulated by a high level of *succinate*, release an attractant *aspartate*, which helps them to aggregate into groups and thus move as concentric patterns of swarms with high bacterial density. The mathematical representation for *E.coli* swarming can be represented by

$$\begin{aligned} J_{cc}(\theta, P(j,k,l)) &= \sum_{i=1}^s J_{cc}^i(\theta, \theta^i(j,k,l)) \\ &= \sum_{i=1}^s \left[-d_{attract} \exp(-w_{attract}) \sum_{m=1}^p (\theta^m - \theta_m^i)^2 \right] \\ &+ \sum_{i=1}^s \left[-h_{repellent} \exp(-w_{repellent}) \sum_{m=1}^p (\theta^m - \theta_m^i)^2 \right] \end{aligned} \quad (51)$$

Where

- J_{cc} - Relative distance of each bacterium from the fittest bacterium
- S - Number of bacteria
- P - Number of Parameters to be optimized

θ^m - Position of the fittest bacteria

$d_{attract}$, $w_{attract}$, $h_{repellent}$, are the coefficients representing the swarming behavior of the bacteria.

10.3. Reproduction

The least healthy bacteria eventually die while each of the healthier bacteria asexually split into two bacteria, which are then placed in the same location. This keeps the swarm size constant. For bacterial, a reproduction step takes place after all chemotactic steps.

$$J^i_{health} = \sum_{j=1}^{N_c+1} J(i, j, k, l) \quad (52)$$

For keep a constant population size, bacteria with the highest J_{health} values die. The remaining bacteria are allowed to split into two bacteria in the same place.

10.4. Elimination and Dispersal

In the evolutionary process, elimination and dispersal events can occur such that bacteria in a region are killed or a group is dispersed into a new part of the environment due to some influence. They have the effect of possibly destroying chemotactic progress, but they also have the effect of assisting in chemotaxis, since dispersal may place bacteria near good food sources. In BFOA, bacteria are eliminated with a probability of P_{ed} . In order to keeping the number of bacteria in the population constant, if a bacterium is eliminated; simply disperse one to a random location on the optimization domain [23].

Problem Formulation

$$Min J = k_2 p_i^2 + k_1 p_i + k_0 \quad (53)$$

Subject to:

$$P_{min} \leq P \leq P_{max} ; Q_{min} \leq Q \leq Q_{max} ; V_{min} \leq V \leq V_{max}$$

Where k_0 , k_1 , k_2 are cost coefficients

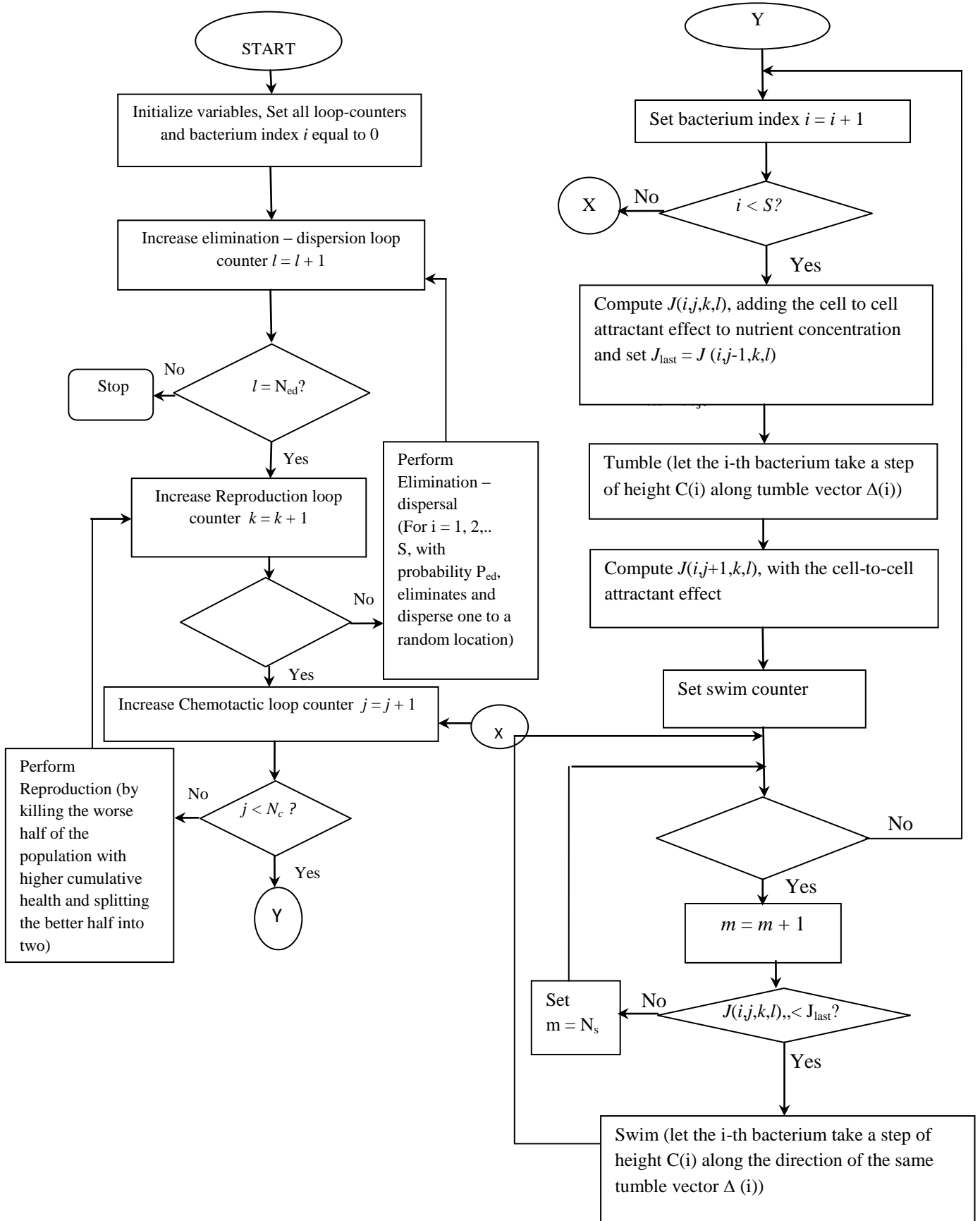


Fig 11: Flowchart of the Bacterial Foraging Algorithm

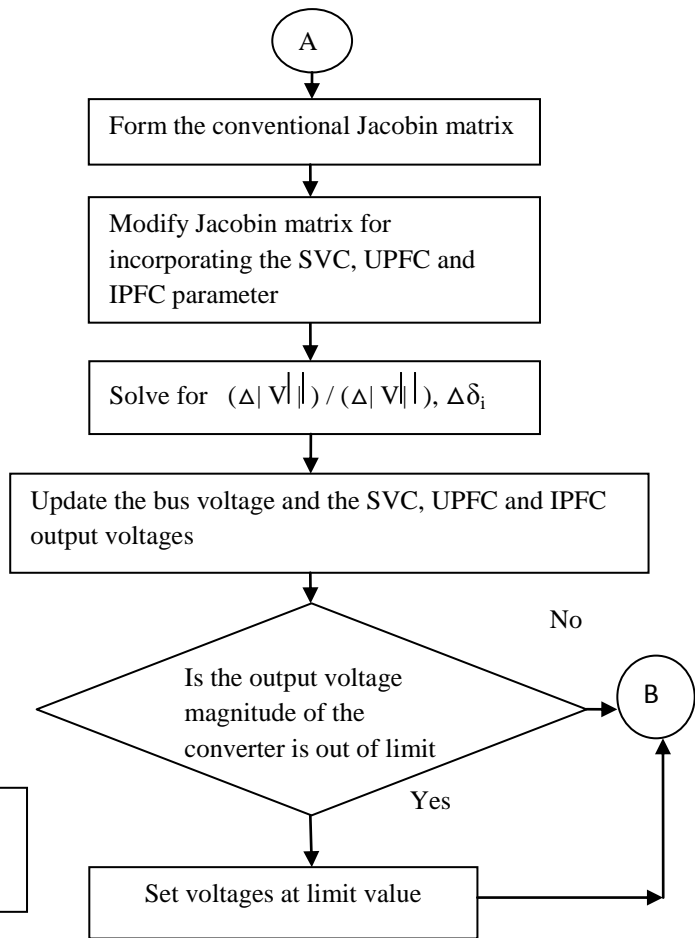
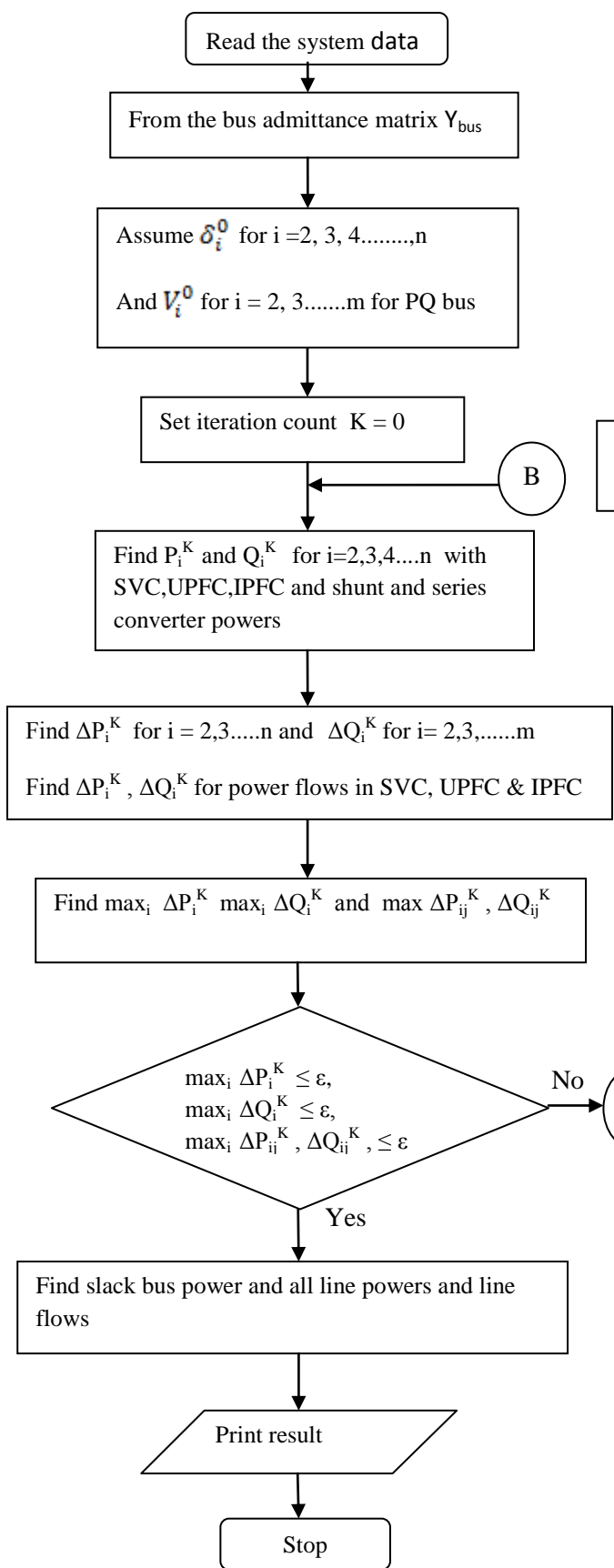


Fig. 12 : Flowchart for the Proposed Method

11.RESULTS

The performance analysis of a IEEE 14-bus, 5-generator system coordinated with different types of Dynamic load models without and with FACTS devices were studied. And the optimum utilization requirement with the FACTS device for each load was determined using BFO technique. In this case of study the buses 5 and 14 are corrected with VDL and ZIP Loads. The system shown as in Fig 13.

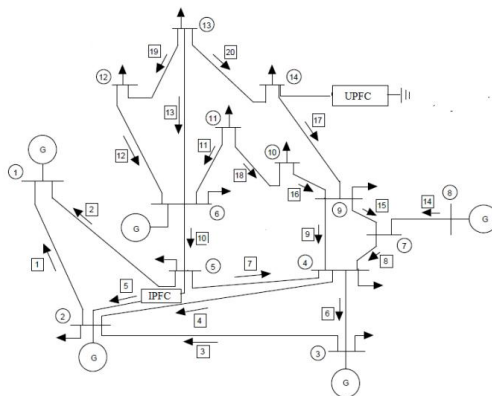


Fig13: IEEE 14-bus test system with FACTS device

Bus No.	Voltage Magnitude	Voltage Angle	Real Power	Reactive Power
1	1.0000	0.0000	2.3630	-0.4339
2	1.0000	-5.385	0.1830	0.6576
3	0.9800	-14.727	-0.9420	0.3087
4	0.9605	-11.637	-0.4780	0.0390
5	0.9619	-9.956	-0.0790	-0.0170
6	1.000	-16.446	-0.1120	0.1105
7	0.9770	-15.090	0.0000	0.0000
8	1.0000	-15.890	0.0000	0.1304
9	0.9614	-16.945	-0.2950	-0.1660
10	0.9601	-17.182	-0.0900	-0.0580
11	0.9760	-16.950	-0.0350	-0.0180
12	0.9821	-17.438	-0.0610	-0.0152
13	0.9750	-17.496	-0.1350	-0.0580
14	0.9715	-18.034	-0.1490	-0.0500

Table.1. Power flow solution for IEEE 14 Bus systems with VDL Load in bus5 and bus 14.

Table. 2. Power flow solution for IEEE 14 Bus systems with ZIP Load in bus 5 and bus 14.

Bus No.	Voltage Magnitude	Voltage Angle	Real Power	Reactive Power
1	1.0000	0.0000	2.3630	-0.4339
2	1.0000	-5.385	0.1830	0.6576
3	0.9800	-14.727	-0.9420	0.3087
4	0.9605	-11.637	-0.4780	0.0390
5	0.9619	-9.956	-0.0790	0.0168
6	1.000	-16.446	-0.1120	0.1105
7	0.9770	-15.090	0.0000	0.0000
8	1.0000	-15.890	0.0000	0.1304
9	0.9614	-16.945	-0.2950	-0.1660
10	0.9601	-17.182	-0.0900	-0.0580
11	0.9760	-16.950	-0.0350	-0.0180
12	0.9821	-17.438	-0.0610	-0.0152
13	0.9750	-17.496	-0.1350	-0.0580
14	0.9393	-30.181	-0.3521	0.0129

Bus No.	SVC				UPFC				IPFC			
	V p.u	Angle	Power at the Bus		V p.u	Angle	Power at the Bus		V p.u	Angle	Power at the Bus	
			MW	MVAR			MW	MVAR			MW	MVAR
1	1.0300	0.00	2.50	0.16	1.0300	0.00	2.50	-0.17	1.0300	0.00	2.50	0.17
2	1.0000	-7.64	0.25	-0.18	1.0000	-7.68	0.25	-0.21	1.0000	-7.67	0.25	0.21
3	1.0000	-19.42	-0.94	0.29	1.0000	-19.31	0.94	0.29	1.0000	19.28	-0.94	0.29
4	1.0000	-16.49	-0.48	0.05	1.0000	-16.22	-0.48	0.04	1.0000	-16.18	-0.48	0.04
5	0.9906	-14.04	-0.06	0.02	0.9915	-13.94	-0.06	0.02	0.9924	-13.97	-0.06	0.02
6	1.0300	-23.43	-0.11	0.01	1.0400	-23.65	-0.11	0.02	1.0500	-23.94	-0.11	0.02
7	1.0042	-21.74	0.00	0.00	1.0049	-21.26	0.00	0.00	1.0055	-21.02	0.00	0.00
8	1.0000	-21.74	0.00	-0.02	1.0000	-21.26	0.00	-0.03	1.0000	-21.02	0.00	-0.03
9	0.9993	-24.56	-0.29	-0.17	1.0005	-21.26	-0.29	-0.06	1.0018	-23.61	0.29	-0.17
10	0.9968	-24.76	-0.09	-0.06	0.9997	-24.29	0.09	-0.17	1.0026	-24.05	-0.09	-0.06
11	1.0095	-24.27	-0.03	-0.02	1.0160	-24.13	-0.03	-0.02	1.0224	-24.14	-0.03	-0.02
12	1.0159	-25.05	-0.06	-0.02	1.0283	-25.43	-0.06	-0.02	1.0412	-25.86	-0.06	-0.02
13	1.0099	-25.62	0.13	0.02	1.0236	-26.26	-0.13	-0.06	1.0384	-26.92	-0.13	-0.06
14	1.0000	-29.83	-0.35	0.2	1.0000	-28.34	-0.36	0.03	1.0000	-27.26	-0.38	0.04

Table.3. Power flow solution for IEEE 14 Bus systems with ZIP Load in Bus 5 and Bus 14 with

Table.4. Power flow solution for IEEE 14 Bus systems with VDL Load in Bus 5 and Bus 14 with various FACTS Devices

Bus No	SVC				IPFC				UPFC			
	V p.u	Angle	Power at the Bus		V p.u	Angle	Power at the Bus		V p.u	Angle	Power at the Bus	
			MW	MVAR			MW	MVAR			MW	MVAR
1	1.0300	0.00	2.27	-0.13	1.0300	- 0.00	2.27	-0.13	1.0300	0.00	2.28	-0.14
2	1.0000	-5.39	0.25	-0.21	1.0000	-5.41	0.25	-0.24	1.0000	-5.41	0.25	-0.25
3	1.0000	-14.17	-0.94	0.30	1.0000	-14.08	-0.94	0.30	1.0000	-14.07	-0.94	0.30
4	1.0000	-9.79	-0.48	0.04	1.0000	-11.41	-0.48	0.04	1.0000	-11.39	-0.48	0.04
5	0.9909	-11.60	-0.06	0.02	0.9920	-9.71	-0.06	0.02	0.9928	-9.75	-0.06	0.02
6	1.0200	-15.88	-0.11	-0.04	1.0300	-15.93	-0.11	0.01	1.0400	-16.19	-0.11	0.01
7	1.0024	-14.85	0.00	0.00	1.0031	-14.56	0.00	0.00	1.0037	-14.41	0.00	0.00
8	1.0000	-14.85	0.00	-0.01	1.0000	-14.56	0.00	-0.02	1.0000	-14.41	0.00	-0.02
9	0.9947	-16.61	-0.29	-0.17	0.9960	-16.25	-0.29	-0.17	0.9972	-16.03	0.29	-0.17
10	0.9913	-16.80	-0.09	-0.06	0.9942	-16.50	-0.09	-0.06	0.9970	-16.36	-0.09	-0.06
11	1.0017	-16.48	-0.03	-0.02	1.0082	-16.35	-0.03	-0.02	1.0146	-16.40	-0.03	-0.02
12	1.0065	-16.89	-0.06	-0.02	1.0165	-16.98	-0.06	-0.02	1.0294	-17.37	-0.06	-0.02
13	1.0030	-17.09	-0.13	-0.06	1.0125	-17.24	-0.13	-0.06	1.0271	-17.82	-0.13	-0.06
14	1.0000	-18.61	-0.12	-0.04	1.0000	-17.85	-0.14	-0.05	1.0000	-17.10	-0.16	-0.07

12. CONCLUSION

This paper presents the coordinated emergency control with the usage of FACTS devices especially (SVC,UPFC,IPFC). It has been found that with the UPFC,IPFC controller, the risk of load shedding is considerably reduced and can easily be adopted for emergency control. Moreover the result indicate that this comparison method successfully prevent the system from blackout and restore the system faster. The Unified Power Flow Controller and Interline Power Flow Controller (UPFC ,IPFC) device can also be replaced for improved reliability as a future work.

APPENDIX

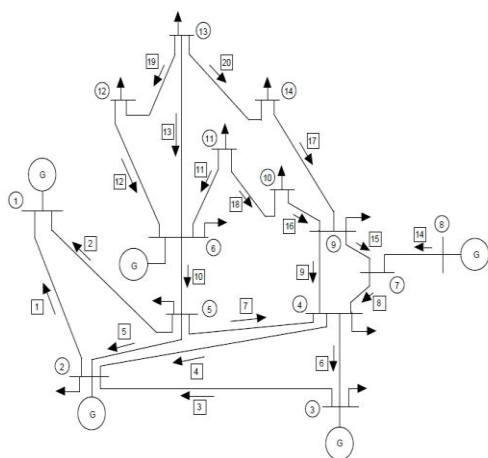


Fig. 14. IEEE 14-bus test system one line diagram

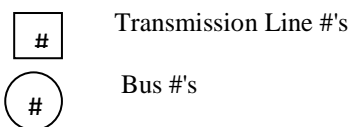


TABLE. 5 .GENERATOR DATA

Generator Bus No.	1	2	3	4	5
MVA	615	60	60	25	25
x_f (p.u.)	0.2396	0.00	0.00	0.134	0.134
r_a (p.u.)	0.00	0.0031	0.0031	0.0014	0.0041
x_d (p.u.)	0.8979	1.05	1.05	1.25	1.25
x'_d (p.u.)	0.2995	0.1850	0.1850	0.232	0.232
x''_d (p.u.)	0.23	0.13	0.13	0.12	0.12
T'_{do}	7.4	6.1	6.1	4.75	4.75
T''_{do}	0.03	0.04	0.04	0.06	0.06
x_q (p.u.)	0.646	0.98	0.98	1.22	1.22
x'_q (p.u.)	0.646	0.36	0.36	0.715	0.715
x''_q (p.u.)	0.4	0.13	0.13	0.12	0.12
T'_{qo}	0.00	0.3	0.3	1.5	1.5
T''_{qo}	0.033	0.099	0.099	0.21	0.21
H	5.148	6.54	6.54	5.06	5.06
D	2	2	2	2	2

TABLE.6. BUS DATA [25]

Bus No.	P Generated (p.u.)	Q Generated (p.u.)	P Load (p.u.)	Q Load (p.u.)	Bus Type*	Q Generated max. (p.u.)	Q Generated min.(p.u.)
1	2.32	-0.169	0.00	0.00	2	10.0	-10.0
2	0.4	0.424	0.2170	0.1270	1	0.5	-0.4
3	0.00	0.234	0.9420	0.1900	2	0.4	0.00
4	0.00	0.00	0.4780	0.0390	3	0.00	0.00
5	0.00	0.122	0.0760	0.0160	3	0.00	0.00
6	0.00	0.00	0.1120	0.0750	2	0.24	-0.06
7	0.00	0.174	0.00	0.00	3	0.00	0.00
8	0.00	0.00	0.00	0.00	2	0.24	-0.06
9	0.00	0.00	0.2950	0.1660	3	0.00	0.00
10	0.00	0.00	0.0900	0.0580	3	0.00	0.00
11	0.00	0.00	0.0350	0.0180	3	0.00	0.00
12	0.00	0.00	0.0610	0.0160	3	0.00	0.00
13	0.00	0.00	0.1350	0.0580	3	0.00	0.00
14	0.00	0.00	0.1490	0.0500	3	0.00	0.00

* Bus Type: 1) Swing bus, 2) Generator bus (PV bus) and 3) Load bus (PQ bus)

TABLE.7. LINE DATA [25]

From Bus	To Bus	Resistance (p.u.)	Reactance (p.u.)	Line charging (p.u.)	Tap ratio
1	2	0.01938	0.05917	0.0528	1
1	5	0.5403	0.22304	0.0492	1
2	3	0.04699	0.19797	0.0438	1
2	4	0.05811	0.17632	0.0374	1
2	5	0.5695	0.17388	0.034	1
3	4	0.6701	0.17103	0.0346	1
4	5	0.01335	0.4211	0.0128	1
4	7	0.00	0.20912	0.00	0.978
4	9	0.00	0.55618	0.00	0.969
5	6	0.00	0.25202	0.00	0.932
6	11	0.099498	0.1989	0.00	1
6	12	0.12291	0.25581	0.00	1
6	13	0.06615	0.13027	0.00	1
7	8	0.00	0.17615	0.00	1
7	9	0.00	0.11001	0.00	1
9	10	0.3181	0.08450	0.00	1
9	14	0.12711	0.27038	0.00	1
10	11	0.08205	0.19207	0.00	1
12	13	0.22092	0.19988	0.00	1
13	14	0.17093	0.34802	0.00	1

TABLE.8. CONTROL PARAMETERS OF THE BACTERIAL FORAGING ALGORITHM

S.No.	Parameters	Values
1	Number of bacteria ,S	45
2	Swimming Length, N _s	4
3	Number of chemotactic steps, N _c	95
4	Number of reproduction steps, N _{re}	4
5	Number of elimination-disperse events, N _{ed}	2
6	Elimination and dispersal Probability, P _{ed}	0.25
7	W _{attract}	0.05
8	W _{repelelnt}	12

9	h _{repelelnt}	0.02
10	d _{attract}	0.02
11	The run-length unit (i.e., the size of the step taken in each run or tumble), C(i)	0.1

TABLE.9. SVC DATA [16]

Parameters	Values
V _{svcm} max	1.1
V _{svcm} min	0.9
G _s	0.9901
B _s	-9.901
Q _s max	0.5
Q _s min	-0.5

13. ACKNOWLEDGEMENT

The authors wish to thank the authorities of Annamalai University, Annamalainagar, Tamilnadu, India for the facilities provided to prepare this paper.

14. REFERENCES

- [1] J. Srivani and K.S. Swarup, "Power system static security assessment and evaluation using external system equivalents," *Electrical Power and Energy Systems*. Vol. 30, pp 83–92, 2 008.
- [2] T. J. Overbye, "A Power Flow Measure for Unsolvable Cases" *IEEE Transactions on Power Systems*, vol. 9, No. 3, pp. 1359–1365, 1994.
- [3] E. Handschin and D. Karlsson, "Nonlinear dynamic load modelling: model and parameter estimation," *IEEE Transactions on Power Systems*, Vol. 11, pp. 1689-1697, 1996.
- [4] J.V. Milanovic and I.A. Hiskens, "The effect of dynamic load on steady state stability of synchronous generator", *Proc.Int. conference on Electric Machines ICEM'94*, Paris, France, 1994.
- [5] W Xu and Y. Mansour, "Voltage stability analysis using generic dynamic load models," *IEEE Transaction Power system*, Vol. 9, No.1, pp. 479-493, 1994.
- [6] D.Karlsson and D.J.Hill, "Modelling and identification of non-linear dynamic load in power systems," *IEEE Transactions on Power Systems*, Vol.9, No. 1, pp. 157-166, 1994.
- [7] S.A.Y. Sabir and D.C. Lee, "Dynamic load models derived from data acquired during system transients", *IEEE Transactions on Power Apparatus and system*, Vol. 101, No.9, pp. 3365-3372, 1982.
- [8] Y. Liang, R. Fischl, A. DeVito and S.C. Readinger, "Dynamic reactive load model," *IEEE Transactions on Power Systems*, Vol.13, No.4, pp.1365-1372, 1998.
- [9] E. Vaahedi, H. El-Din, and W. Price, "Dynamic load modeling in large scale stability studies," *IEEE Transactions on Power Systems*, Vol. 3, No. 3, pp. 1039–1045, 1988.
- [10] Xiao, Y., Song, Y.H., Liu, C.C. and Sun, Y.Z., "Available transfer capability enhancement using FACTS devices", *IEEE Transactions on Power Systems*, Vol. 18, No. 1, pp.305-312, 2003.

- [11] C. A. Canizares and Z. T. Faur, "Analysis of SVC and TCSC controllers in voltage collapse," *IEEE Transactions on Power Systems*, Vol. 14, No. 1, pp. 158–165, 1999.
- [12] R. Palma-Behnke, L. S. Vargas, J. R. Pérez, J. D. Núñez and R. A. Torres, "OPF with SVC and UPFC modeling for longitudinal systems," *IEEE Transactions on Power Systems*, vol. 19, no. 4, pp. 1742–1753, 2004.
- [13] M. A. Abido, "Power System Stability Enhancement Using FACTS Controllers: A Review", *The Arabian Journal for Science and Engineering*, Vol. 34, No 1B, pp 153-172, 2009.
- [14] Padiyar, K.R and Kulakarni, A.M, "Control Design and Simulation of Unified Power Flow Controller," *IEEE Transactions on Power Systems*, Vol.13, No.4, pp.1348-1354, 1998.
- [15] Huang, Z., N. Yixin, C.M. Shen, F.W. Felix, S. Chen and B. Zhang, "Application of UPFC in interconnected power systems - modelling, interface, control strategy and case study," *IEEE Transactions on Power Systems*, Vo. 15 (2), pp. 817-824, 2000.
- [16] H.Fujita, Y.Watanabe, H. Akagi, "Control and Analysis of a Unified Power Flow Controller," *IEEE Transactions on Power Electronics* Vol.14, No.6, 1999.
- [17] Prakash G. Burade, and Jagdish B. Helonde, "Dynamic Modelling of UPFC Optimum Tuning by Using Hybrid Artificial Intelligent Controller." *International Journal of Research and Reviews in Electrical and Computer Engineering*, Vol. 1, No. 4, pp.1040-1046, 2011.
- [18] Jianhong Chen, Tjing T. Lie, and D.M. Vilathgamuwa, "Basic control of interline power flow controller," *Proc. of IEEE Power Engineering Society Winter Meeting*, New York, USA, Jan. 27-31, pp.521-525, 2002.
- [19] Y. Zhang, C. Chen, and Y. Zhang, "A Novel Power Injection Model of IPFC for Power Flow Analysis Inclusive of Practical Constraints," *IEEE Transactions on Power Systems*, Vol. 21, No. 4, pp. 1550 – 1556, 2006.
- [20] Babu, A.V.N, and Sivanagaraju, S, "Mathematical modelling, analysis and effects of Interline Power Flow Controller (IPFC) parameters in power flow studies," *IEEE Transactions on Power Systems*, Vol. 19, pp. 1-7, 2011.
- [21] Rahmat Allah Hooshmand, and Mostafa Ezatabadi Pour, "Corrective action planning considering FACTS allocation and optimal load shedding using bacterial foraging oriented by particle swarm optimization algorithm," *Turk J Elect. Eng. & Comp. Sic*, Vol.18, No.4, 2010.
- [22] M. Tripathy and S. Mishra, "Bacteria Foraging-based Solution to optimize both real power loss and voltage stability limit," *IEEE Transactions on Power Systems*, Vol. 22, No. 1, pp. 240-248, 2007.
- [23] Panigrahi B.K., and Pandi V.R., "Congestion management using adaptive bacterial foraging algorithm", *Energy Conversion and Management*, Vol. 50, No.5, pp. 1202-1209, 2009.
- [24] S. K. M. Kodsí and C. A. Cañizares, "Modeling and Simulation of IEEE14 bus System with FACTS

Controllers", Technical Report, University of Waterloo, 2003.

- [25] M.A. Pai, *Computes Techniques in Power System Analysis*, Tata McGraw Hill Potholing Co, New Delhi, 1986.

15.AUTHORS PROFILE

I.A.Chidambaram (1966) received Bachelor of Engineering in Electrical and Electronics Engineering (1987), Master of Engineering in Power System Engineering (1992) and Ph.D in Electrical Engineering (2007) from Annamalai University, Annamalaiagar. During 1988 - 1993 he was working as Lecturer in the Department of Electrical Engineering, Annamalai University and from 2007 he is working as Professor in the Department of Electrical Engineering, Annamalai University, Annamalaiagar. He is a member of ISTE and ISCA. His research interests are in Power Systems, Electrical Measurements and Control Systems. (Electrical Measurements Laboratory, Department of Electrical Engineering, Annamalai University, Annamalaiagar – 608002, Tamilnadu, India, Tel: - 91-04144-238501, Fax: -91-04144-238275) driacdm@yahoo.com

T.A. Rameshkumar (1973) received Bachelor of Engineering in Electrical and Electronics Engineering (2002), Master of Engineering in Power System Engineering (2008) and he is working as Assistant Professor in the Department of Electrical Engineering, Annamalai University, Annamalaiagar. He is currently pursuing Ph.D degree in Electrical Engineering from Annamalai University. His research interests are in Power Systems, Control Systems, and Electrical Measurements. (Electrical Measurements Laboratory, Department of Electrical Engineering, Annamalai University, Annamalaiagar - 608 002, Tamilnadu, India, tarpagutharivu@gmail.com)